A. Kaestner :: Paul Scherrer Institut

Introduction to computed tomography

Theory and practical details for the experimentalist

Outline

Introduction

Learning objectives

- Understand the image formation process
- Understand the differences between analytical and iterative reconstruction
- Knowing key parameters in tomographic reconstruction and how they impact the resulting images
- Recognizing typical artifacts and how to remove them

The problem

We have a solid item to investigate. . .

- For a first look of the outside

- Cut the item in pieces

- Next step, use a transmission image

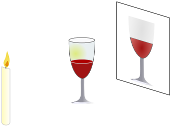

Different sources to illuminate the sample

X-rays

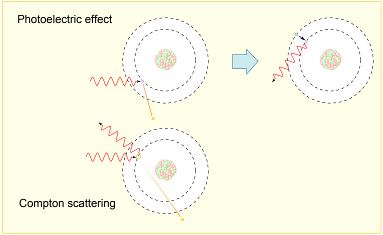

- Electromagnetic radiation.
- Interaction with the electron shells.

Neutrons

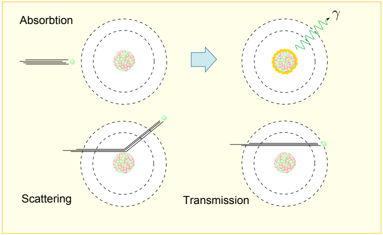

- Neutral particle beam.
- Interaction with the nucleus.

A ray illuminates a semi-transparent medium

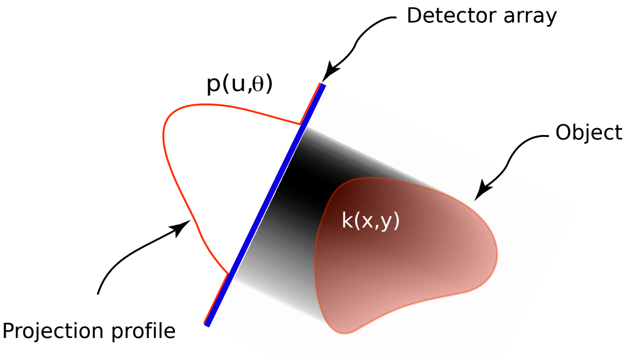

Transmission imaging – Radiography

A ray penetrating a medium is attenuated according to Beer-Lamberts law The intensity is attenuated in the medium according to

$$I = I_0 e^{\int_L k(x,y)\, dl}$$

- I - Intensity behind the sample
- I_0 - Incident intensity
- k - Attenuation coefficient,
  - μ - Linear attenuation coefficient X-rays
  - Σ - Macroscopic cross-section for neutrons
- L - Line through the sample.

Computing an attenuation image

From Beer-Lamberts law we get

$$p = -\log\left(\frac{r - r_{DC}}{r_{OB} - r_{DC}}\right) = -\log$$

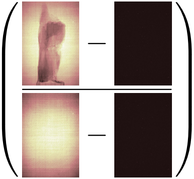

$$=$$

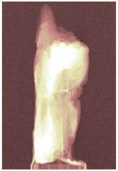

p	Normed projection
r	Measured radiogram
r_{DC}	Dark current image (removes noise floor)
r_{OB}	Open beam image, measured I_0

Each pixel represent the line integral $\int_L k(x)dx$ through the sample.

Generalized attenuation law 1D

Piecewise constant sample

Few discrete regions

$$I = I_0\, e^{-\sum_{i=1}^{N} k_i\, x_i}$$

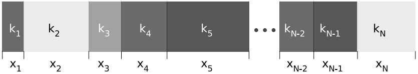

Continuous samples

Let $x_i = \Delta x$ and $\Delta x \to 0$

$$I = I_0\, e^{-\int_L k(x)\, dx}$$

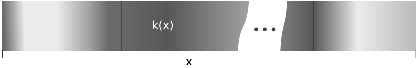

Attenuation coefficients

X-rays at 150keV

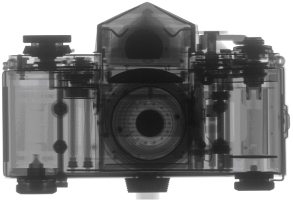

Group → / ↓Period	1	2	3	4	5	6	7	8	9	10	11	12	13	14	15	16	17	18
1	H 0.02																	He 0.02
2	Li 0.06	Be 0.22											B 0.28	C 0.27	N 0.11	O 0.16	F 0.14	Ne 0.17
3	Na 0.13	Mg 0.24											Al 0.38	Si 0.33	P 0.25	S 0.30	Cl 0.23	Ar 0.20
4	K 0.14	Ca 0.26	Sc 0.48	Ti 0.73	V 1.04	Cr 1.29	Mn 1.32	Fe 1.57	Co 1.78	Ni 1.96	Cu 1.97	Zn 1.64	Ga 1.42	Ge 1.33	As 1.50	Se 1.23	Br 0.90	Kr 0.73
5	Rb 0.47	Sr 0.86	Y 1.61	Zr 2.47	Nb 3.43	Mo 4.29	Tc 5.06	Ru 5.71	Rh 6.08	Pd 6.13	Ag 5.67	Cd 4.84	In 4.31	Sn 3.98	Sb 4.28	Te 4.06	I 3.45	Xe 2.53
6	Cs 1.47	Ba 2.73		Hf 19.70	Ta 25.47	W 30.49	Re 34.47	Os 37.92	Ir 39.01	Pt 38.61	Au 35.94	Hg 25.88	Tl 23.23	Pb 22.81	Bi 20.28	Po 20.22	At -	Rn 9.77
7	Fr -	Ra 11.80		Rf -	Db -	Sg -	Bh -	Hs -	Mt -	Ds -	Rg -	Uub -	Uut -	Uuq -	Uup -	Uuh -	Uus -	Uuo -
Lanthanides				La 5.04	Ce 5.79	Pr 6.23	Nd 6.46	Pm 7.33	Sm 7.68	Eu 5.66	Gd 8.69	Tb 9.46	Dy 10.17	Ho 10.17	Er 11.70	Tm 12.49	Yb 9.32	Lu 14.07
Actinides				Ac 24.47	Th 28.95	Pa 39.65	U 49.08	Np -	Pu -	Am -	Cm -	Bk -	Cf -	Es -	Fm -	Md -	No -	Lr -

Thermal neutrons

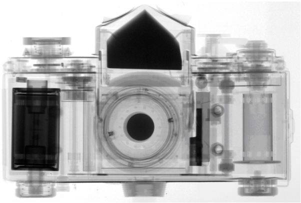

Group → / ↓Period	1	2	3	4	5	6	7	8	9	10	11	12	13	14	15	16	17	18
1	H 3.44																	He 0.02
2	Li 3.30	Be 0.79											B 101.6	C 0.56	N 0.43	O 0.17	F 0.20	Ne 0.10
3	Na 0.09	Mg 0.15											Al 0.1	Si 0.11	P 0.12	S 0.06	Cl 1.33	Ar 0.03
4	K 0.06	Ca 0.08	Sc 2.00	Ti 0.60	V 0.72	Cr 0.54	Mn 1.21	Fe 1.19	Co 3.92	Ni 2.05	Cu 1.07	Zn 0.35	Ga 0.49	Ge 0.47	As 0.67	Se 0.73	Br 0.24	Kr 0.61
5	Rb 0.08	Sr 0.14	Y 0.27	Zr 0.29	Nb 0.40	Mo 0.52	Tc 1.76	Ru 0.58	Rh 10.88	Pd 0.78	Ag 4.04	Cd 115.1	In 7.58	Sn 0.21	Sb 0.30	Te 0.25	I 0.23	Xe 0.43
6	Cs 0.29	Ba 0.07		Hf 4.99	Ta 1.49	W 1.47	Re 6.85	Os 2.24	Ir 30.46	Pt 1.46	Au 6.23	Hg 16.21	Tl 0.47	Pb 0.38	Bi 0.27	Po -	At -	Rn -
7	Fr -	Ra 0.34		Rf -	Db -	Sg -	Bh -	Hs -	Mt -	Ds -	Rg -	Uub -	Uut -	Uuq -	Uup -	Uuh -	Uus -	Uuo -
Lanthanides				La 0.52	Ce 0.14	Pr 0.41	Nd 1.87	Pm 5.72	Sm 171.47	Eu 94.58	Gd 1479.0	Tb 0.93	Dy 32.42	Ho 2.25	Er 5.48	Tm 3.53	Yb 1.40	Lu 2.75
Actinides				Ac -	Th 0.59	Pa 8.46	U 0.82	Np 9.80	Pu 50.20	Am 2.86	Cm -	Bk -	Cf -	Es -	Fm -	Md -	No -	Lr -

[Sears, 1992]

Some attenuation examples for neutrons

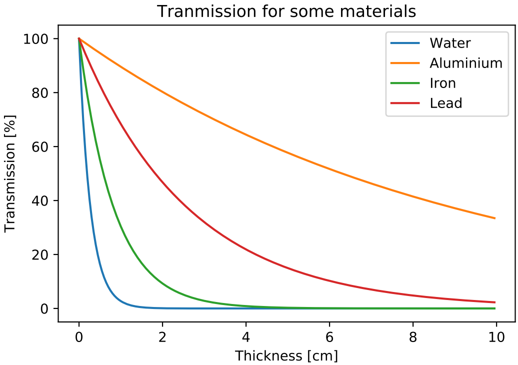

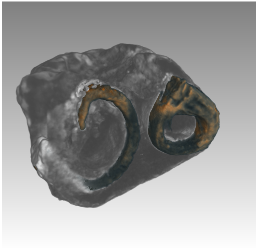

Neutron tomography of fist-sized lead canon ball from the battle of Bossworth (1485AD)

Limitation of the radiography

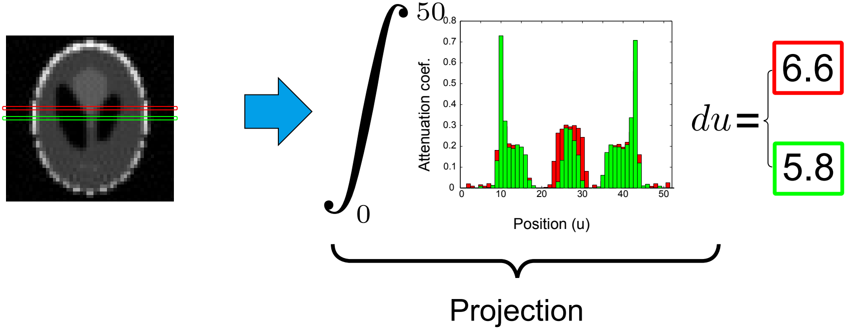

- Great local changes buried in the sum of bulk
- Depth position can’t be determined

Stereography

Use two projections at 90° to get depth information

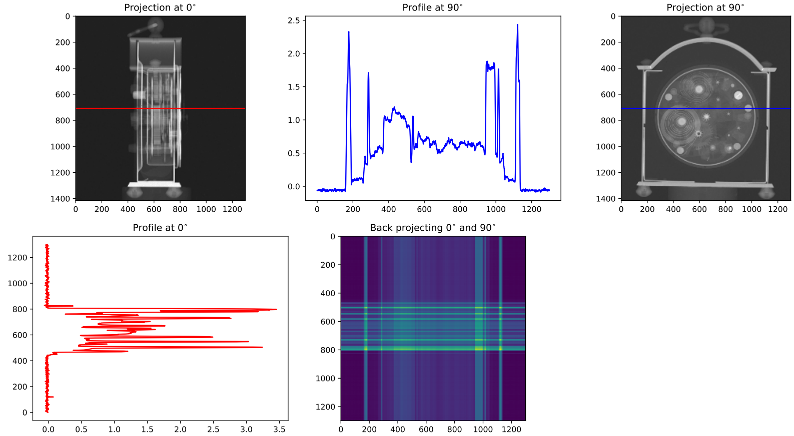

- Provides some depth information
- Still a lot of guessing

The solution is not unique

Single projection → several solutions

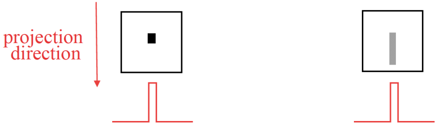

Two projections → several solutions

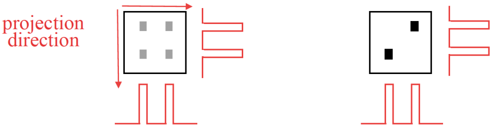

A unique solution would exist only for an infinite number of noiseless continuous projections

What is tomography?

- A method to capture three-dimensional images.
- An indirect method using projections (radiograms) to reconstruct the inner structure of a sample.
- Free translation is slice imaging
  from Greek:

  Tomos – ’a section’ or ’a cutting’
  Graph – write

History

1917 **Radon** developed the foundation for the inversion required by tomography.

1956 **Bracewell** the relationships between Fourier transform and Radon transform.

1963 First applications to medical tomography. **Kuhl** obtained first backprojection. **Cormack** applied Radon's results to radiograms.

1970 Publication of the first CT image.

1970-1973 **Cormack** & **Hounsfield** first CT scanner.

1979 **Cormack** & **Hounsfield** the Nobel prize in Medicine.

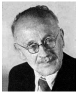

J. Radon (1887–1956)

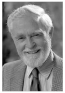

R. Bracewell (1921–2007)

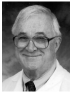

D Kuhn (1929–2017)

A. Cormack (1924–1998)

Sir G.N. Hounsfield (1919–2004)

Inspecting the sample from different views

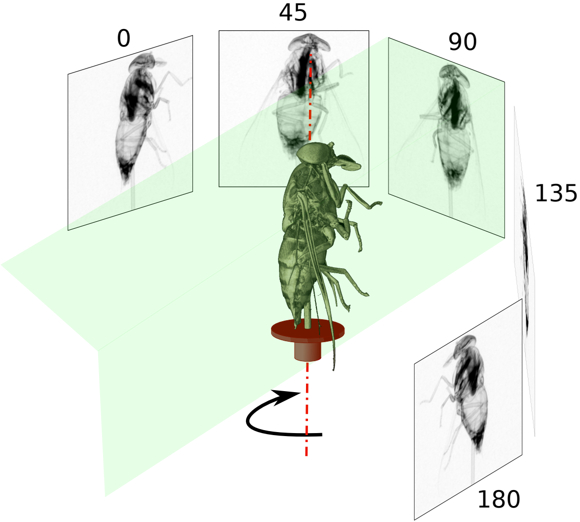

A first attempt to reconstruction: Algebraic solution

Observations

$$\begin{array}{ccl} 2 & 3 & \rightarrow 5 \\ 1 & 4 & \rightarrow 5 \\ \downarrow & \downarrow & \\ 3 & 7 & \end{array}$$

Equation system

$$\begin{aligned} a_{11}x_1 + a_{12}x_2 &= y_1 \\ a_{21}x_3 + a_{22}x_4 &= y_2 \\ a_{11}x_1 + a_{21}x_3 &= y_3 \\ a_{12}x_2 + a_{22}x_4 &= y_4 \\ &\vdots \end{aligned}$$

$$\Rightarrow A\,x = y$$

Solve the equation system for x

Many equations, sparse matrix A, no unique solution...

A first attempt to reconstruction: Back-projection

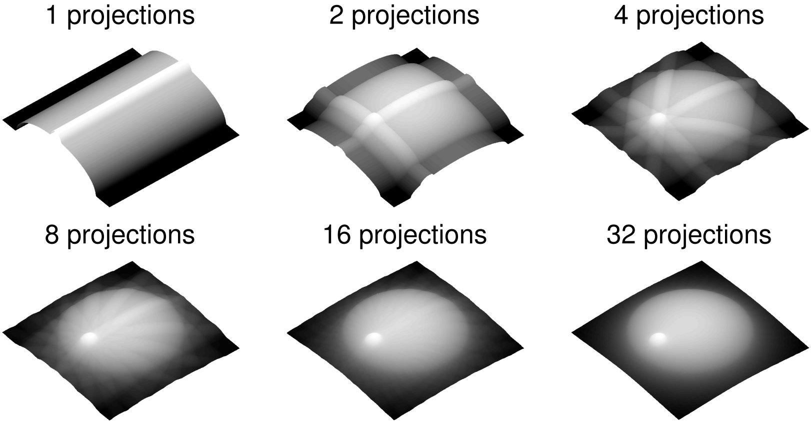

The solution is too smooth…something is missing!!!

Reconstruction

The reverse process – reconstruction

The scanning provides projection data…

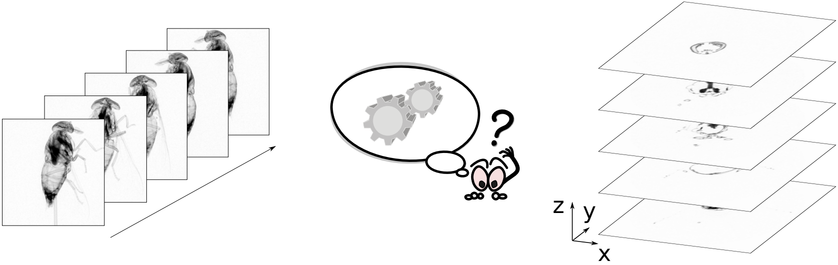

…but we want to find the cross section which caused the projection.

> *We have to find the inverse Radon transform or solve the equation system $A\,x = y$*

Sinogram construction

Combine take the same line from all projections into a new image

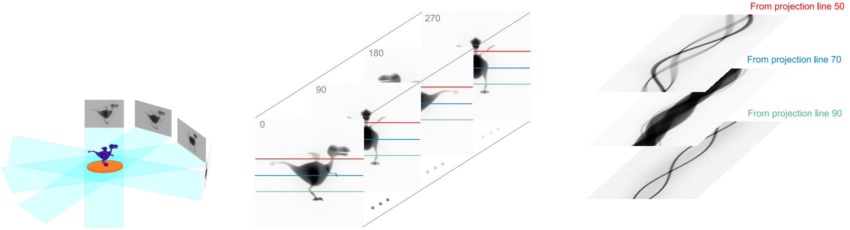

The information required to reconstruct a single slice.

Looking at the sinogram

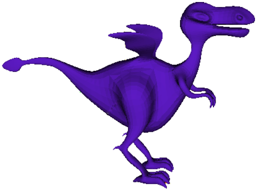

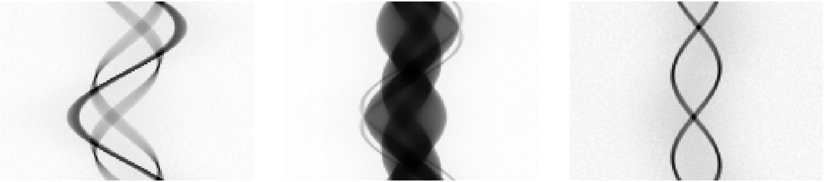

The Radon Transform and the sinogram

Projection and sinogram

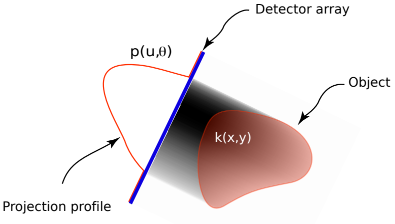

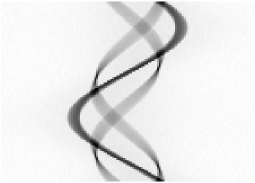

The Radon transform

An analytical description of projection I acquired at angle θ

$$p = \underbrace{-\ln\left(\frac{I(u,\theta)}{I_0(u)}\right)}_{\text{Measured}} = \int_{-\infty}^{\infty} \underbrace{k(x,y)}_{\text{Wanted}} \underbrace{\delta(x\ \cos\ \theta + y\ \sin\ \theta - u)}_{\text{Observation ray}}\, dx\, dy$$

[Radon, 1917]

Inversion – Fourier slice theorem

Theorem

The Fourier transform of a parallel projection $p(x)$ of an object $f(x, y)$ obtained at an angle θ equals a line through origin in the 2D Fourier transform of $f(x, y)$ at the same angle.

$$f(x) = \int_{-\infty}^{\infty} f(x,y)\, dy$$

$$f(\xi) = \int_{-\infty}^{\infty}\int_{-\infty}^{\infty} f(x,y)\, e^{-j2\pi\xi x}\, dx\, dy$$

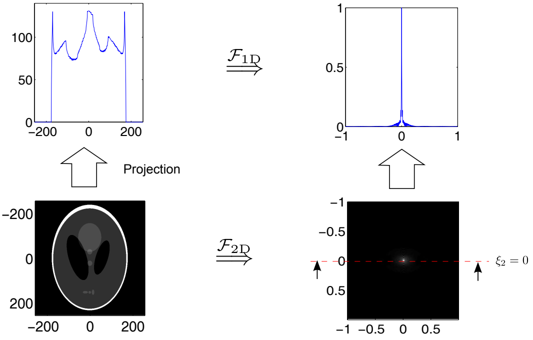

$$f(x,y)$$

$$F(\xi_1,\xi_2) = \int_{-\infty}^{\infty}\int_{-\infty}^{\infty} f(x,y)\, e^{-j2\pi\,(x\xi_1 + y\xi_2)}\, dxdy$$

[Bracewell, 1956]

Analytical solution

Reconstruction in the frequency domain

$$k(x,y) = \int_0^{\pi} \int_{-\infty}^{\infty} |\omega| P(\omega,\theta)\, e^{j2\pi\omega(x\cos\theta + y\sin\theta)}\, d\omega d\theta$$

Reconstruction in the spatial domain

$$k(x,y) = \frac{1}{2\pi^2} \int_0^{\pi} \int_{-\infty}^{\infty} \underbrace{\partial p/\partial u(u,\theta)}_{\textit{Convolution}} \underbrace{[x\cos\theta + y\sin\theta - u]^{-1}}_{\textit{Rotation}}\, du d\theta$$

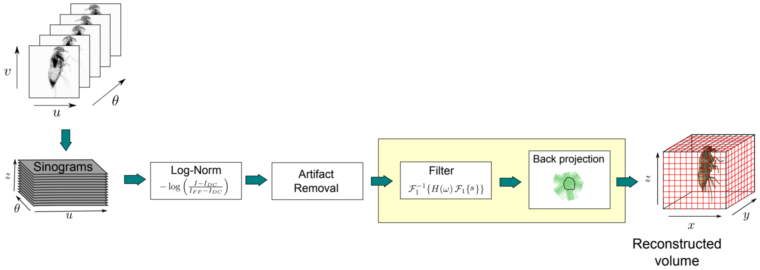

Some line integrals in the sinogram

The value of a single pixel is given by the line integral along a sine.

Sinogram

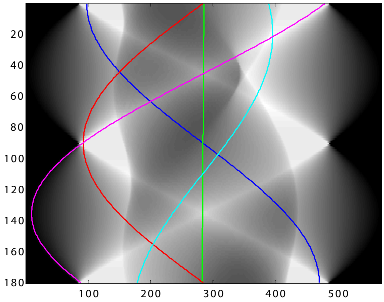

Cross section

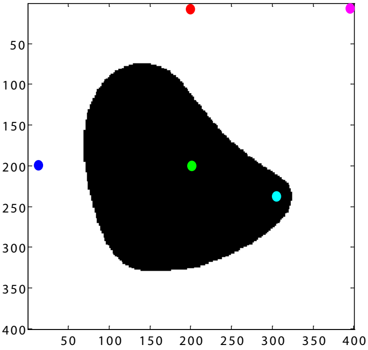

The reconstruction filter

Reconstruction in the spatial domain

$$k(x,y) = \frac{1}{2\pi^2} \int_0^{\pi} \int_{-\infty}^{\infty} \underbrace{\partial p / \partial u(u,\theta)}_{Convolution} \underbrace{\left[x \cos\theta + y \sin\theta - u\right]^{-1}}_{Rotation} \, du d\theta$$

The filter

The filter has two components:

- A derivative: $\partial p / \partial u(u,\theta) \equiv \mathcal{F}^{-1}(|\omega| \cdot \mathcal{F}(p))$
- Apodization: Shepp-Logan, Hamming, *etc*

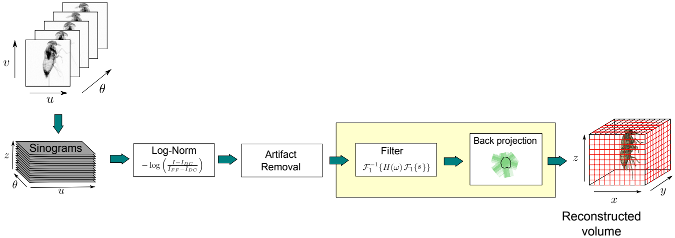

Reconstruction filter in action

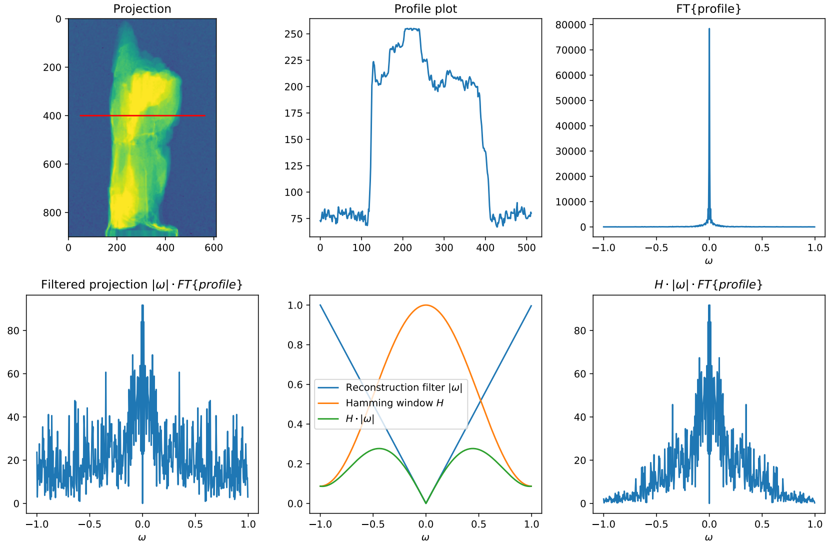

PAUL SCHERRER INSTITUT

The effect of the reconstruction filter

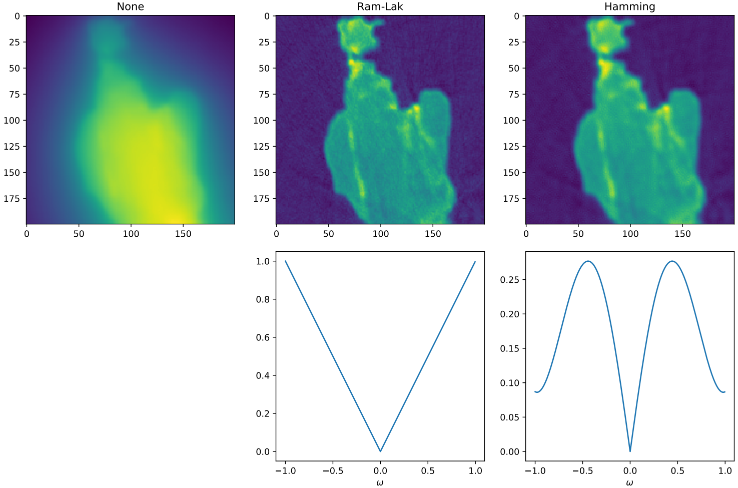

Apodization filters suppress noise and blur edges

When the analytical solution has problems

Few projections

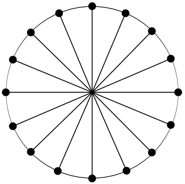

Irregularly distributed

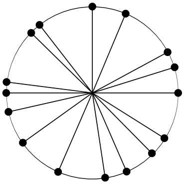

Limited view

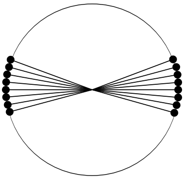

Low SNR or contrast

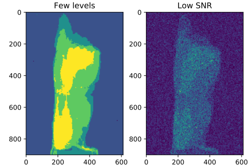

Iterative methods overview

Algebraic methods

- ART
- SIRT
- TV
- etc...

Statistical methods

- Maximum likelihood
- Penalized ML
- etc..

Pros & cons

+ Sparse, irregularly sampled projection data
  - Limited angle
  - Few views
+ Physical model can be included
- Requires prior information for best performance.
- Time consuming

Why iterative inversion

Building the system matrix

$$\begin{aligned} a_{11}x_1 + a_{12}x_2 + \ldots &= y_1 \\ a_{21}x_3 + a_{22}x_4 + \ldots &= y_2 \\ a_{11}x_1 + a_{21}x_3 + \ldots &= y_3 \\ &\vdots \end{aligned}$$

$$\begin{bmatrix} a_{11} & \cdots & a_{1N} \\ \vdots & \ddots & \vdots \\ a_{N1} & \cdots & a_{NN} \end{bmatrix} \begin{bmatrix} x_1 \\ \vdots \\ x_N \end{bmatrix} = \begin{bmatrix} y_1 \\ \vdots \\ y_N \end{bmatrix}$$

Example

You have:

- 1000 projections which are 1000 pixels wide
- The reconstructed slice has 1000×1000

This gives $1000 \times 1000 \times 1000 = 10^9$ equations
$\rightarrow$ A is a $10^9 \times 10^9$ matrix!

Some features of A

- Sparse matrix
- Ill-posed (ideally infinitely many equations needed)
- Inversion doesn't provide unique solution

Algebraic Reconstruction Method (ART)

Problem to solve

We want to solve the equation $A\,x = y$,
where A is the forward projection operator, a large sparse matrix

Kaczmarz method (ART)

$$x^{k+1} = x^k + \lambda_k \frac{y_i - \langle a_i, x^k \rangle}{\|a_i\|^2}\, a_i$$

- a_i the i^{th} row of the system matrix A.
- x^k the reconstructed image at the k^{th} iteration.
- y_i the i^{th} element of the sinogram
- λ_k relaxation parameter

Statistic reconstruction methods

Problem to solve

We want to solve the equation $A\,x = y + noise$,

Iteration scheme

Maximize likelihood function:

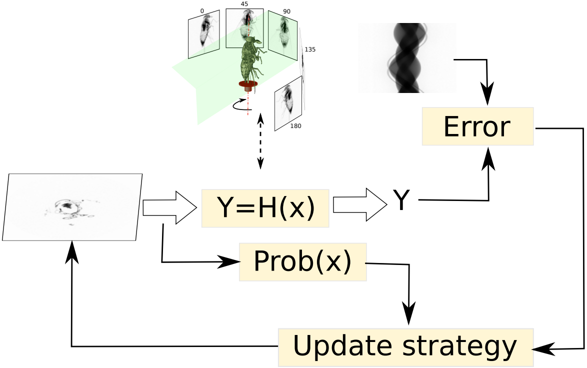

Beam geometry

Different beamline configurations

Static beamline

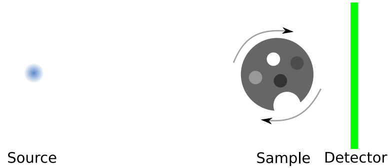

Rotating beamline

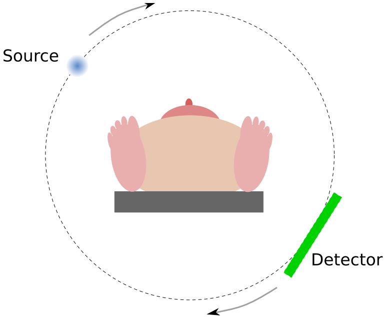

PAUL SCHERRER INSTITUT

Pencil-beam

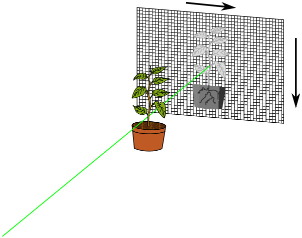

- Simples beam geometry
- Single pixels are scanned
- The 'Hounsfield-approach'

Parallel beam

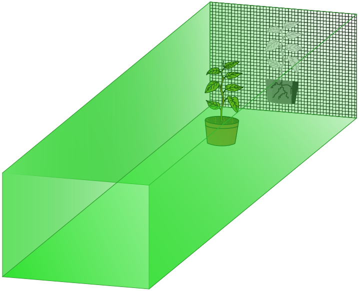

- Produces 2D projections
- No geometric unsharpness
- Simple reconstruction, filtered back projection [Buzug, 2008]

Fan beam

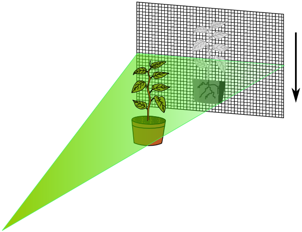

- Line-wise scan
- Beam incidence must be perpendicular to detector plane
- Magnifying in one direction

Cone beam

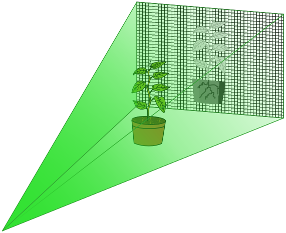

+ Uses 2D-projections.
+ Magnifying due to beam divergence.
- Non-trivial reconstruction using [Feldkamp et al., 1984].
- Only in the central slice is exact.

Problems with cone-beam

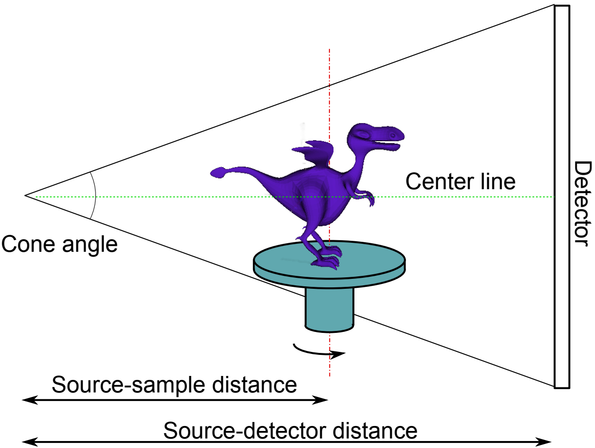

Parallel discs

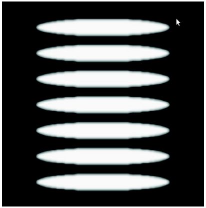

FDK (cone angle 30°)

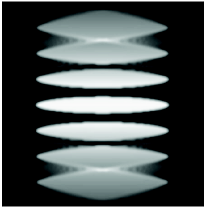

Neutron imaging – Pin hole geometry

Penumbra blurring

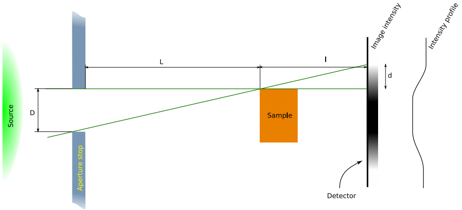

Collimation ratio

The width of the penumbra blurring is described by the collimation ratio:

$$\frac{L}{D} = \frac{l}{d}$$

L Distance from aperture to sample

D Width of aperture diameter

l Distance from sample to detector

d Width of unsharpness

Beam divergence

Typical collimation ratio L/D = 100 – 2000 [mm/mm]

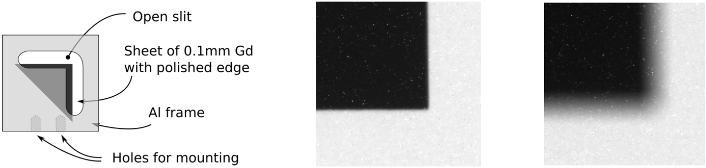

(a) (b) (c)

Fig 3. Schematic of the edge sample (a) and neutron radiographs obtained with the sample at 3mm (b) and 320mm (c) away from the detector. The edge unsharpness is mainly caused by penumbra blurring.

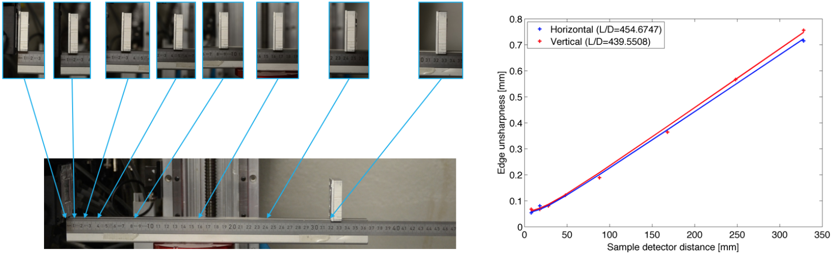

Fig 4. It is possible to estimate the collimation ratio by measuring the edge unsharpness at different distances from the detector.

[Kaestner et al., 2017]

The impact of beam divergence

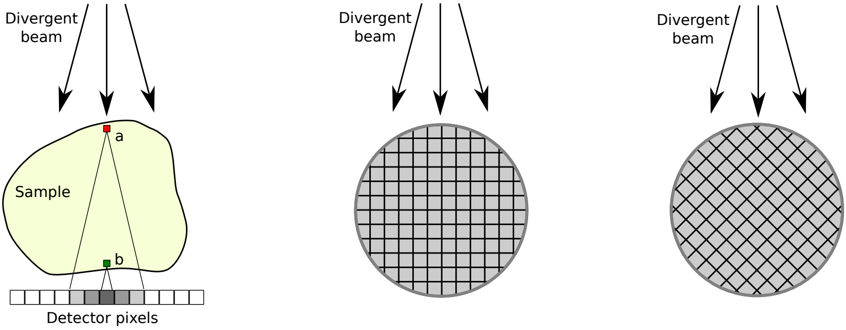

Improved results using CBCT reconstruction

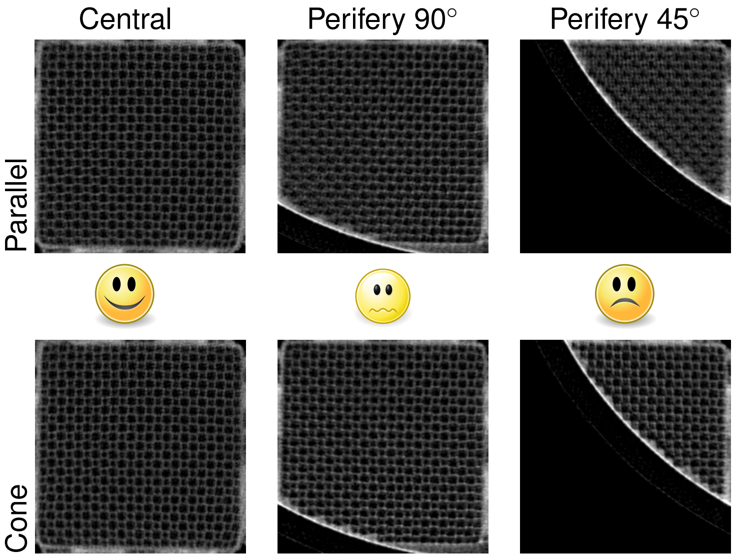

[Kaestner et al., 2012]

Helical scans

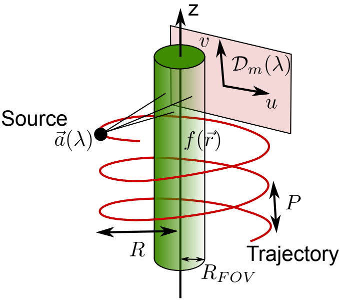

- Exact 3D solution
- Long objects
- Reconstruction using Katsevich[Katsevich, 2002]

Large samples – The problem

Requirement

Projections from at least 180° + sample must always be visible.

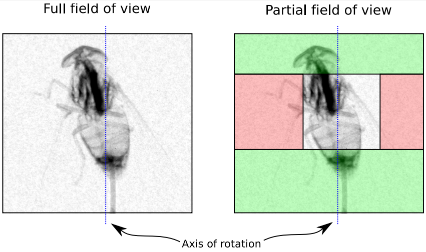

Two options to handle samples larger than the field of view

- Translate the COR and use a 360° orbit.
- Truncated reconstruction

Translated projections

Idea

- Translate the COR to the side of the projection
- Near doubled FOV

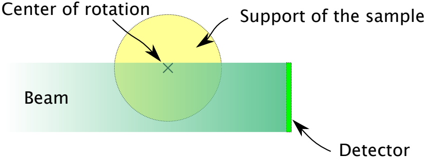

Requirements

- The projections must be stitched
- Projections must be acquired over 360°
- More voxels requires more projections

Truncated or Local tomography

A truncated tomography has incomplete data support.

Effects of truncation

1. Some attenuation information is missing $\rightarrow$ bias
   The shadow contains more attenuation than the projection data shows.
2. Truncation gives spikes on the edges.
   The derivative in the reconstruction formula produce edge artifacts.

Removing truncation artifacts

Origin The derivative of the truncated edge is steep

Solution Add a smooth transition from edge to zero

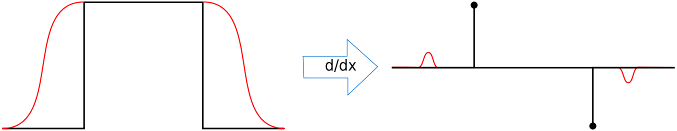

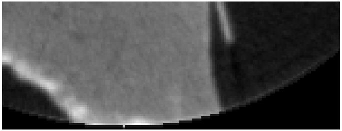

Original

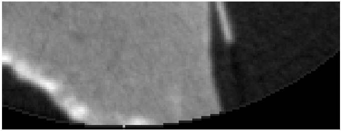

Padded

Position of the acquisition axis

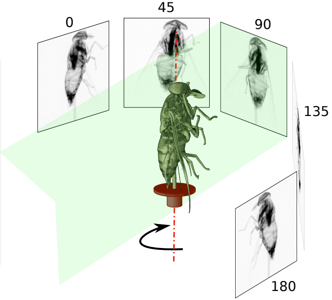

The axis

The point where all rays intersect is called the center of rotation for a single slice or the rotation axis for many slices. This point must be provided to the reconstructor.

Centering artifacts

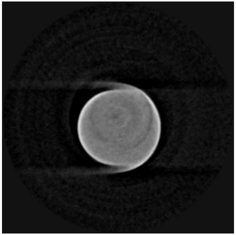

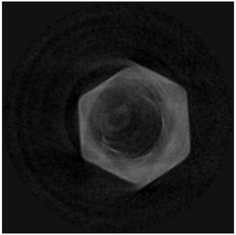

The impact of center misalignment

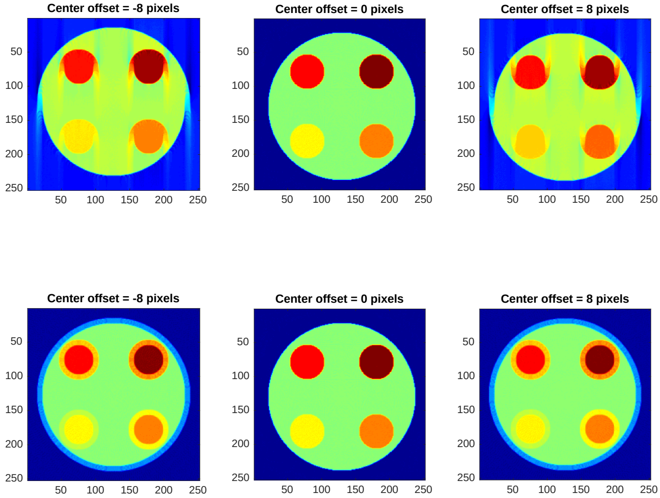

The finding center

Projection data

- Mirror one projection
- Translate until they overlap
- Center = midpoint + translation distance

Reconstructed data

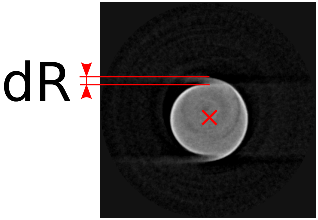

center = current $\pm$ dR/2

Tilted sample or table

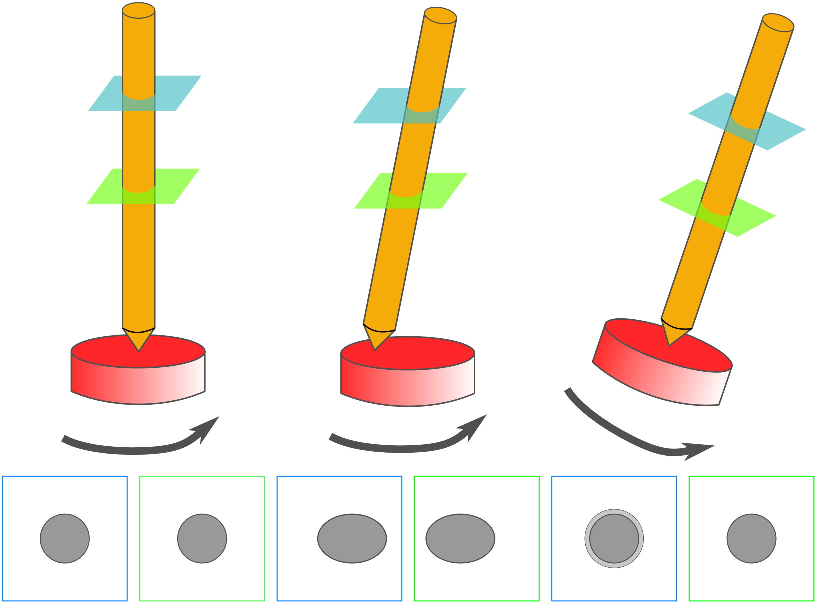

Tilted acquisition axis

Along the beam

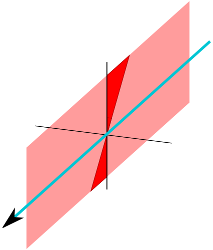

- Hard to correct
- Requires vector based reconstructor and geometry

Across the beam

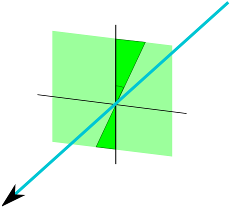

Small angles corrected with COR shifts

Large angles corrected with rotation

Sampling

Discretizing the reconstruction formula

The inversion formula is impractical since it would require infinite amount of equations to solve.

- The projections are digital images
  - Intensity sampling [bits/pixel]
  - Spatial sampling [pixels/mm]
- The rotation is done in steps
- The reconstruction is done on a finite matrix

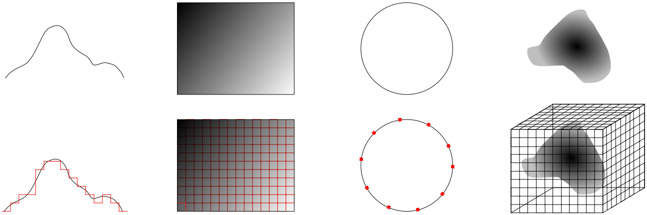

How many projections are needed?

The number of projections is determined by the sampling theorem [Buzug, 2008].

$$N_{projections} = \frac{\pi}{2} N_u$$

N_u Number of pixels in the direction perpendicular to the axis of rotation.

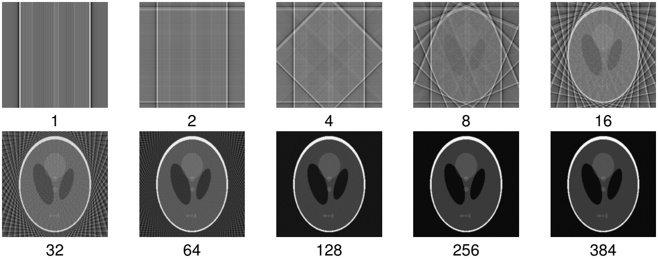

Intuitive proof of the sampling theorem

Basic idea The unit circle in the Fourier domain must be filled.

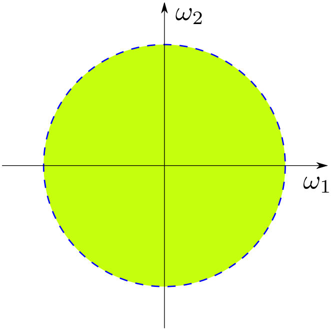

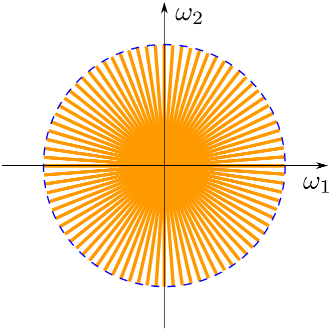

Noise and Dose

Noise

Noise is an additive statistical phenomenon.

$\mathcal{R}^{-1}\{$ 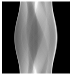 $\} + \mathcal{R}^{-1}\{$ 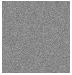 $\} = \mathcal{R}^{-1}\{$  $\} \rightarrow$ 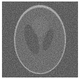

Noise sources:

- Thermal noise from the electronics.
- Algorithmic, rounding errors, interpolation model etc.
- Noise induced by the radiation source.

Dose

The dose is the amount of radiation events hitting the detector.
More events improve the SNR (the law of great numbers).

Noise, exposure time, and number of projections

The noise level of a slice is directly connected to the dose used. The dose is defined as

$$\textit{Dose} = \textit{Flux} \times \textit{Time}$$

The signal to noise ratio can be improved by increasing

- the beam intensity,
- the exposure time,
- the number of projections,
- detector exchange.

What influences the contrast?

$$C_{slice}\, W_{sample} \sim C_{projection}\, N_{projections}$$

C_{slice}	Slice contrast
$C_{projection}$	Projection contrast (Open beam - darkest region)
$N_{projections}$	Number of projections
W_{sample}	Largest width of the sample in pixels

Contrast experiment

The phantom

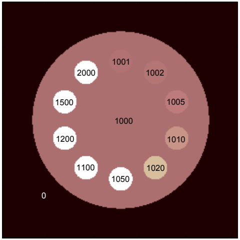

Parameters

- w=192
- $N_{projections}$=288
- $C_{projection}$=6, 7, 8, 9, 10,11, 12, 13 bits
- Contrast ratio: 1000:1, . . . , 1:2
- Noise free

What can be seen?

Changing projection contrast with constant number of projections

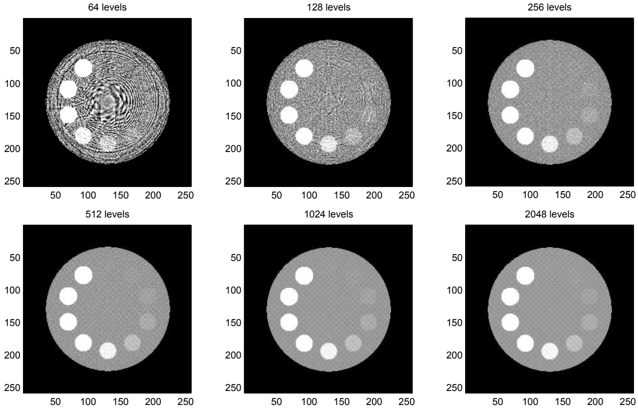

The reconstruction noise decrease with increasing dynamics

Artefacts

Common artefacts

Rings are caused by stuck or dead pixels. They have the same value for all projections

Lines are caused by single pixels or groups pixels in a single projection

High contrast these artifacts appear as star-like streaks originating from the high contrast object.

Motion when the sample changes during acquisition.

Beam hardening Polychromatic beam

Scattering The beam is scattered

Ring artifacts

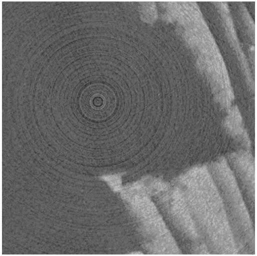

- Ring artefacts are very common in tomography.
- They are caused by a stuck, dead, or hot pixels.
- They appear as:
  - Lines in the sinogram
  - Concentric rings in the CT slices

Correction in the Radon space

Projections Identify and remove spots that persists through projections.

Sinograms Identify lines parallel to the θ-axis

- Subtract first derivative of average projection form sinogram.
- Filter sinogram in Fourier domain (notch filter or wavelet filter).

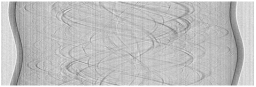

$-$

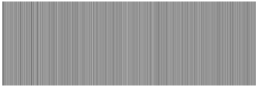

$=$

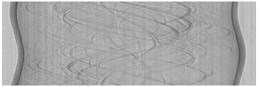

$s(u,\theta)$

$\mathbf{1}^T \cdot (E_u[s] - median_N(E_u[s]))$

Correction in the matrix

Correction procedure:

- Transform matrix to polar coordinates
- Detect lines
- Make replacement map
- Transform map to Carthesian coordinates
- Correct matrix

Advantage Good for testing different strengths

Disadvantage The coordinate transformations

Line artifacts

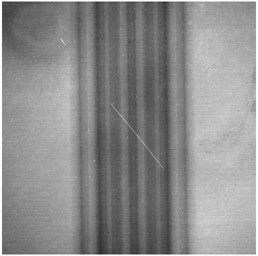

Projection

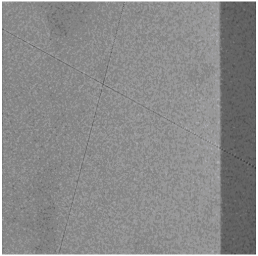

Reconstructed slice

- Line artifacts are more common with neutrons
- The origin of a line is a local spot in the sinogram.
- The orientation and position depends on when the spot was registered.

Correction of the lines

Correction method

- Detect the spots on the projections – compute local variances
- Replacement *e.g.*
  $p_{corrected} = w(\sigma) \cdot p + (1 - w(\sigma)) \cdot p_{median}$ with $0 \leq w \leq 1$

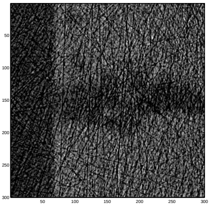

Raw

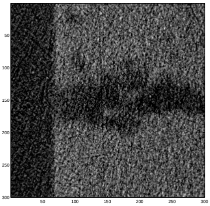

Corrected

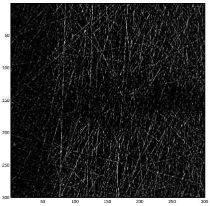

Difference

Motion artifacts

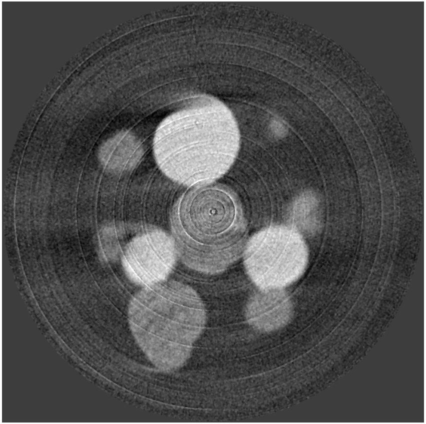

Sequential acquisition

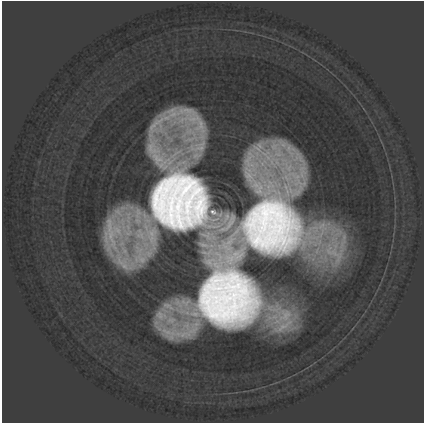

Golden ratio acquisition

Suppressing the effect of motion

Dynamic processes are hard to observe with CT

- CT needs long scan times.
- If the interfaces move more than 1 pixel during the scan motion artifacts will appear.

The solution

- Increment the acquisition angle by the Golden ratio $\phi = \frac{1+\sqrt{5}}{2}$
- The sample will always be observed at 'orthogonal' angles.

[Köhler, 2004, Kaestner et al., 2011]

Cupping

Definition

Cupping is a phenomenon that appears as a drop of attenuation coefficients in large homogeneous bodies. The main origins are:

Beam hardening
: when the radiation attenuation depends on energy.

Scattering
: background scattering adds a bias.

Cupping due to Beam hardening

The attenuation depends on energy

Monochromatic

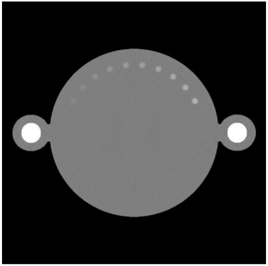

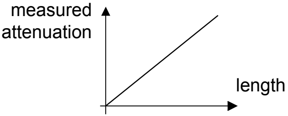

Polychromatic

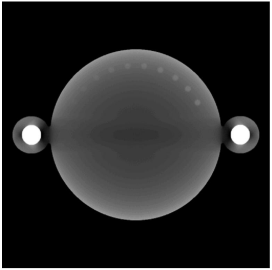

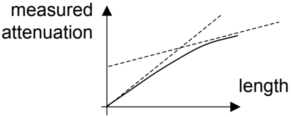

Attenuation for neutrons

The attenuation law assumes the intensity to be absorbed…

This is not true for neutrons!!!

Most neutrons are scattered

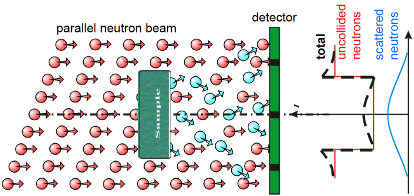

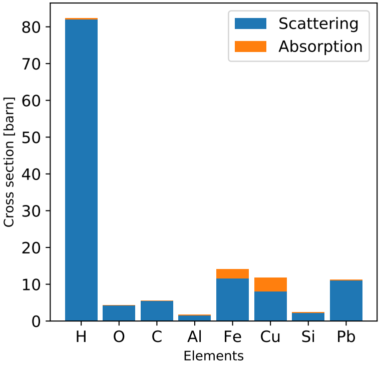

Background and sample scattering

Scattered neutrons are bad for

- Quantitative imaging
- Segmentation algorithms

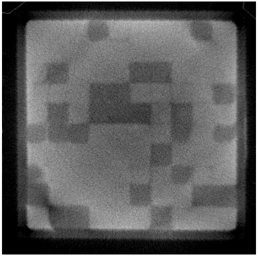

Uncorrected

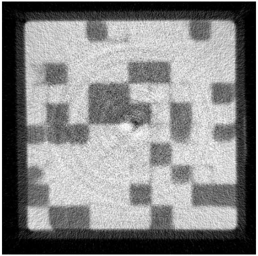

Corrected by QNI [Hassanein, 2006]

Scattering correction next generation

Measurements

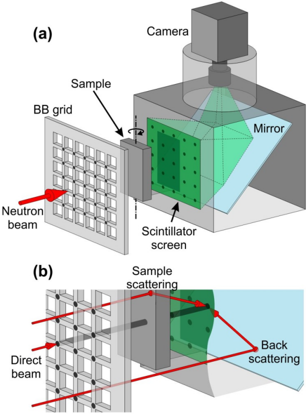

Correction and result

- Estimate scattering profile using black bodies.
- Correction using revised projection normalization

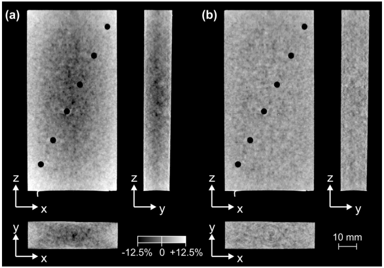

[Boillat et al., 2018]

Demonstrating the effect of BB correction

Samples: Cylinders of bone. Scanned at ICON.

Normalized

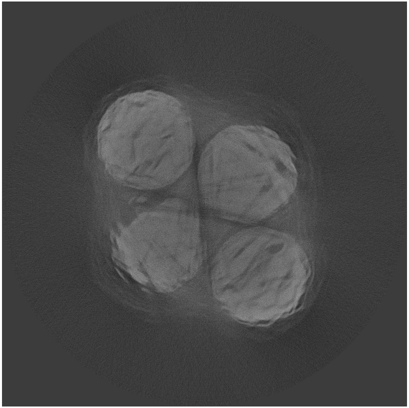

Scatter corrected with BB

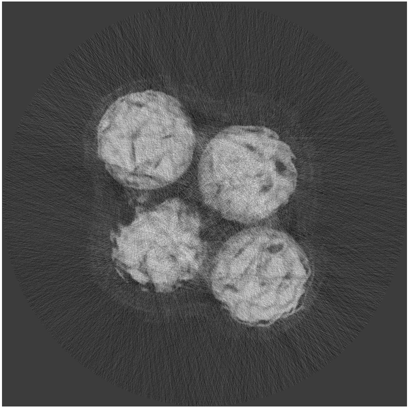

Data courtesy of E. Törnquist, Lund University

Summary

PAUL SCHERRER INSTITUT

Summary

- Tomography is an indirect acquisition method
- Different sources can be used
- The perfect tomography needs
  - many projections
  - well illuminated projections
- Artifacts may and will appear but can mostly be corrected.

Questions

I'm done

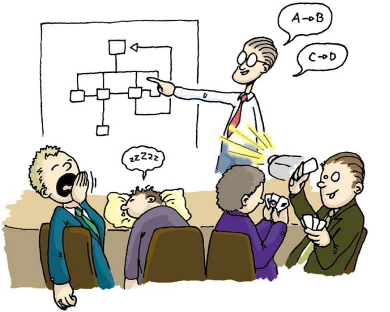

Your turn

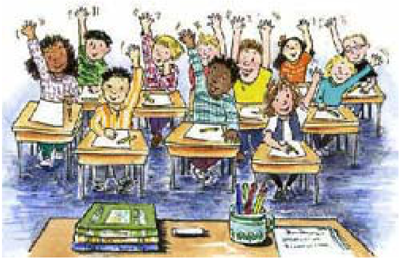

Filtered back-projection (Proof)

Image function:

$$f(x,y) = \int_{-\infty}^{\infty}\int_{-\infty}^{\infty} F(\xi_1,\xi_2)\, e^{j2\pi(x\xi_1+y\xi_2)}\, d\xi_1 d\xi_2$$

Coordinate transform $\{\xi_1,\xi_2\} = \{\omega\cos\theta, \omega\sin\theta\}$

$$f(x,y) = \int_{0}^{2\pi}\int_{-\infty}^{\infty} F(\omega\cos\theta, \omega\sin\theta)\, e^{j2\pi\omega(x\cos\theta+y\sin\theta)}\, d\omega d\theta$$

Fourier slice theorem:

$$f(x,y) = \int_{0}^{2\pi}\int_{-\infty}^{\infty} P(\omega,\theta)\, e^{j2\pi\omega(x\cos\theta+y\sin\theta)}\omega\, d\omega d\theta$$

Symmetry properties:

$$P(\omega,\theta+\pi) = P(-\omega,\theta)$$

Rotated coordinates:

$$f(x,y) = \int_{0}^{\pi}\int_{-\infty}^{\infty} P(\omega,\theta)\, e^{j2\pi\omega(x\cos\theta+y\sin\theta)}|\omega|\, d\omega d\theta$$

A basic back-projection algorithm

```
pProj  : pointer to line in sinogram
pSlice : pointer to slice matrix

for (float line=0; line<nProjections; line++) {                  // Loop over projections in s
    for (size_t y=0; y<SizeY; y++) {                            // Loop over matrix in y
        const size_t cfStartX = mask[y].first;                  // Get x-coordinates
        const size_t cfStopX  = mask[y].second;
        fStartU += cos(theta[line]);                            // Compute first proj. pos.
        float fPosU=fStartU-sin(theta[line])*cfStartX;

        for (size_t x=cfStartX; x<cfStopX; x++) {               // Loop over matrix in x
            int nPosU=static_cast<int>(fPosU-=sin(theta[line]));  // Compute position

            const float interpB=fPosU-nPosU;                    // Interpolation weight right
            const float interpA=1.0f-interpB;                   // Interpolation weight left

            pSlice[x+y*sizeX]+=interpA*pProj[nPosU]+interpB*pProj[nPosU+1];
        }
    }
}
```

References I

Boillat, P., Carminati, C., Schmid, F., Grünzweig, C., Hovind, J., Kaestner, A., Mannes, D., Morgano, M., Siegwart, M., Trtik, P., Vontobel, P., and Lehmann, E. (2018).
Chasing quantitative biases in neutron imaging with scintillator-camera detectors: a practical method with black body grids.
Optics Express, 26(12):15769.

Bracewell, R. (1956).
Strip integration in radio astronomy.
Australian Journal of Physics, 9(2):198.

Buzug, T. (2008).
Introduction to Computed Tomography: From photon statistics to modern cone-beam CT.
Springer.

Feldkamp, L., Davis, L., and Kress, J. (1984).
Practical cone-beam algorithm.
J. Opt Soc. Am. A, 1(6):612–619.

Hassanein, R. (2006).
Correction methods for the quantitative evaluation of thermal neutron tomography.
Diss. eth no. 16809, Swiss Federal Institute of Technology.

Kaestner, A., Grünzweig, C., and Lehmann, E. (2012).
Improved analysis techniques for new applications in neutron imaging.
In *Proc 18th World Conference on Nondestructive Testing*, pages 1–10.

Kaestner, A., Kis, Z., Radebe, M., Mannes, D., Hovind, J., Grünzweig, C., Kardjilov, N., and Lehmann, E. (2017).
Samples to determine the resolution of neutron radiography and tomography.
Physics Procedia, 88:258–265.

References II

Kaestner, A., Münch, B., Trtik, P., and Butler, L. (2011).
Spatio-temporal computed tomography of dynamic processes.
Optical Engineering, 50(12):123201.

Katsevich, A. (2002).
Theoretically exact filtered backprojection-type inversion algorithm for spiral ct.
SIAM Journal on Applied Mathematics, 62(6):2012–2026.

Köhler, T. (2004).
A projection access scheme for iterative reconstruction based on the golden section.
In *Nuclear Science Symposium Conference Record*, volume 6, pages 3961–3965. IEEE.

Radon, J. (1917).
Ueber die bestimmung von funktionen durch ihre Integralwerte tangs gewisser mannigfaltigkeiten.
Berichte Saechsisch Akad. Wissenschaften (Leipzig), Math. Phys., Klass 69:262–277.

Sears, V. (1992).
Neutron scattering lengths and cross sections.
Neutron News, 3(3):26–37.